RESEARCH ARTICLE

The neural correlates of value representation: From single items to bundles

Jekaterina Zyuzin[1] | Dalton Combs[1] | John R. Monterosso[2] | Isabelle Brocas[3]

[1]University of Southern California, Los Angeles, California, USA

[2]Department of Psychology, University of Southern California, Los Angeles, California, USA

[3]Department of Economics, University of Southern California, Los Angeles, California, USA

Correspondence
Isabelle Brocas, Department of Economics, University of Southern California, 3620 S. Vermont Avenue, Los Angeles 90089-0001, USA.
Email: brocas@usc.edu

Abstract

One of the core questions in Neuro-economics is to determine where value is represented. To date, most studies have focused on simple options and identified the ventromedial prefrontal cortex (VMPFC) as the common value region. We report the findings of an fMRI study in which we asked participants to make pairwise comparisons involving options of varying complexity: single items (Control condition), bundles made of the same two single items (Scaling condition) and bundles made of two different single items (Bundling condition). We construct a measure of choice consistency to capture how coherent the choices of a participant are with one another. We also record brain activity while participants make these choices. We find that a common core of regions involving the left VMPFC, the left dorsolateral prefrontal cortex (DLPFC), regions associated with complex visual processing and the left cerebellum track value across all conditions. Also, regions in the DLPFC, the ventrolateral prefrontal cortex (VLPFC) and the cerebellum are differentially recruited across conditions. Last, variations in activity in VMPFC and DLPFC value-tracking regions are associated with variations in choice consistency. This suggests that value based decision-making recruits a core set of regions as well as specific regions based on task demands. Further, correlations between consistency and the magnitude of signal change with lateral portions of the PFC suggest the possibility that activity in these regions may play a causal role in decision quality.

KEYWORDS
bundles, choice consistency, fMRI, revealed preferences, subjective value

1 | INTRODUCTION

Evidence from many lesion and fMRI studies converge in identifying the medial orbitofrontal cortex (MOFC) or sometimes more narrowly, the ventromedial prefrontal cortex (VMPFC) as a critical region in valuation when deciding between alternatives (Fellows & Farah, 2007; Henri-Bhargava et al., 2012; Lee et al., 2021; Rangel et al., 2008) or how much to pay for a good or item (Chib et al., 2009; Hare

et al., 2008; Plassmann et al., 2007). This finding has been consistently reported in studies involving food items, trinkets, and money (Bartra et al., 2013; Clithero & Rangel, 2013b; Levy & Glimcher, 2012). Most studies however have focused on choices involving single items, as opposed to complex options made of several single items, or bundles. Among the few studies involving bundles, the VMPFC has been associated with the ability to make consistent choices between bundles (Camille et al., 2011) and the MOFC has been shown to reflect the

difference in subjective value between monetary options and bundled options (FitzGerald et al., 2009). In other forms of complex options, such as multi-attribute options, activity in the VMPFC reflected also the value of the combined items (Kahnt et al., 2011; Pelletier et al., 2021).

A recent study reported that our ability to make choices consistent with one another depends critically on the complexity of options (Brocas et al., 2019a). Participants evidenced more inconsistency when making a series of choices between bundles involving three items compared with choices between bundles involving two items. This increased inconsistency was linked to working memory and it was found more significant in older adults. It seems intuitive that complex options are difficult to evaluate. If the constituent items of a bundle are valued sequentially, working memory, which is responsible for the short-term mental maintenance and manipulation of information, may be required to hold values prior to integration. If a person is required to consume a bundle they choose, value calculations must take into account not only the value of constituents but also any externality of consuming them together. Such task may not differ from other difficult tasks that rely on executive function.

Studies have demonstrated that activation is evoked in the dorsolateral prefrontal cortex (DLPFC) during tasks that tax executive function (Baker et al., 1996; Berman et al., 1995; Goel et al., 1997; Goldberg et al., 1998; Nichelli et al., 1994; Osherson et al., 1998; Petrides, 1994). Activation studies have shown that dorsal frontal regions are activated during tasks that are experienced as difficult (Braver et al., 1997; Cohen et al., 1994, 1997; Luo et al., 2012; Monterosso et al., 2007), and during task switching (Dove et al., 2000), and the DLPFC is differentially recruited as tasks become more complex (Baker et al., 1996; Braver et al., 1997; Carlson et al., 1998; Christoff et al., 2001; Cohen et al., 1997; Demb et al., 1995). This relationship extends to tasks requiring the explicit representation and manipulation of knowledge, where the ability to reason relationally is essential (Kroger et al., 2002). The DLPFC is also implicated in evidence accumulation in perceptual decisions and is differentially activated across easy and complex decisions (Heekeren et al., 2004, 2006).

The role of DLPFC in value-based decision making has not been clearly established. It is sometimes reported to be activated and, when it is reported, its involvement is interpreted in the context of the question of interest. For instance, the DLPFC has been found to encode the variability of multi-attribute objects (Kahnt et al., 2011) and to be more active when trade-offs between attributes are required (McFadden et al., 2015). In food choices, the DLPFC has been reported to modulate value (Camus et al., 2009; Chen et al., 2018; Gluth et al., 2012; Hare et al., 2011a, 2011b; Sokol-Hessner et al., 2012) and craving (Fregni et al., 2008; Hall et al., 2017), to be involved in self-regulation and self-control (Chen et al., 2018; Harris et al., 2013; Hutcherson et al., 2012), and to be associated with eating disorders (Brooks et al., 2011; Dalton et al., 2020; Foerde et al., 2015; He et al., 2019; Lowe et al., 2019). It has also been linked to addictive behavior (Koob & Volkow, 2010; Nakamura-Palacios et al., 2016). The DLPFC has also been found to be functionally connected with the value coding regions in self-control paradigms (Hare et al., 2009) and in multi-attribute paradigms (Rudorf & Hare, 2014). Taken together, the evidence places the DLPFC at the core of value-based decision making when multiple dimensions (e.g., taste, health, future outcomes) must be integrated to form subjective value (Brocas & Carrillo, 2021). Last, the DLPFC is significantly more active when options involve a conflict to be resolved (Baumgartner et al., 2011; de Wit et al., 2009). Taken together, these findings suggest that a potential role of DLPFC is to support value calculation (perhaps in various ways) when choices are complex.

Here, we report the results of an fMRI study in which participants were asked to choose between real food options involving single item options and bundled items options. Bundles varied in complexity and consisted of either the same two single items or two different single items. In each condition, we constructed a measure of consistency to reflect how coherent choices were with one another. Because we were not interested in down regulation or dysfunctions of the value system, we only recruited participants who did not have any food restrictions and were not on a diet. We also excluded junk food. We hoped to replicate the standard results obtained in the literature in the case of single items comparisons and to study the differential effect of bundling. Given the evidence reported earlier, we hypothesized that bundles made of different items would require more cognitive effort to be evaluated and greater choice consistency would be linked to DLPFC activity. Bundling made of the same two options were introduced to control for quantity effects. We were specifically interested in neural activity and value-tracking as a function of decision complexity. For this reason, participants were always asked to choose between one option, that varied across trials, and a fixed (reference) option (a design similar to Hare et al. (2009)). We specifically tracked activity associated with the computation of the subjective value of the varying option. Our design allows us to address the following questions: (1) Is there a common value tracking region when options are simple and complex? (2) What are the neural correlates of subjective value as a function of the complexity of items (single, scaled or bundled)? (3) Does valuation of multiple goods recruit networks implicated in attention and working memory? and (4) Do consistent choices across conditions have a neural signature?

2 | MATERIALS AND METHODS

2.1 | Subjects

Sixty eight healthy young adults (mean age 22 years old, 36 female and 32 male, all right-handed) were recruited from the Los Angeles Behavioral Economics Laboratory's subject pool at the University of Southern California. The Institutional Review Board of USC approved the study. Subjects could participate if they satisfied the standard eligibility criteria for fMRI studies (no cognitive disorder or psychiatric condition, no medication affecting cognition, no history of seizure, and no metal implants). We excluded subjects who reported to have food allergies, food restrictions or to be picky eaters. All participants

received a $50 show-up fee for participating. They were also rewarded with one of their choices, selected randomly at the end of the session. Eight participants were excluded because of incomplete data collection or excessive head movement during scanning.

2.2 | Procedure

Participants were instructed to not eat for at least 4 h before the experimental session. They were also instructed that they would have to stay after the session to consume what they had obtained and that they could not take any of the food items with them when they leave. This was implemented to make sure participants were hungry and thinking carefully about their choices during the session. The procedure was explained beforehand so that each participant knew that their reward would be based on their choices, and they should make their best decision in every trial.

Each participant was asked to rank 30 single item options by order of preference. Each option was a small food serving. All were calibrated to represent between 20 and 50 calories and to look visually similar. The actual servings were displayed in the experimental room. Participants were given cards, each showing the picture of one serving, and they ranked options by placing cards on a long table. This ranking was used to create 40 bundles, 20 combinations of two same single items, and 20 combinations of two different single items. The participant was then asked to include those bundles in their previous ranking. Asking participants to rank all options allowed us to abstract from nonlinearity effects (complementarity or substitutability between single items) when value was combined. We then selected 11 single item options, 10 combinations of two same single items and 10 combinations of two different single items to include in the experimental task, where each participant made binary choices in the scanner. One of the 11 single item options was a reference option, denoted hereafter by REF. Choices were divided into three conditions (see Figure 1a): CONTROL, SCALING, and BUNDLING. Each participant made choices in all three conditions. In each of the CONTROL trials, the participant had to choose between REF and one of the 10 remaining single items. In each of the SCALING trials, the participant had to choose between REF and one of the 10 combinations of two same single items. In each of the BUNDLING trials, the participant had to choose between REF and one of the 10 combinations of two different single items. SCALING trials were included to control for the effect of quantity. In all cases, REF was off-screen, it was the same for each trial and it was shown to the participant at the beginning of the experiment. The other option was on-screen and it was displayed at the beginning of each trial (see Figure 1b). Each individual trial was repeated nine times
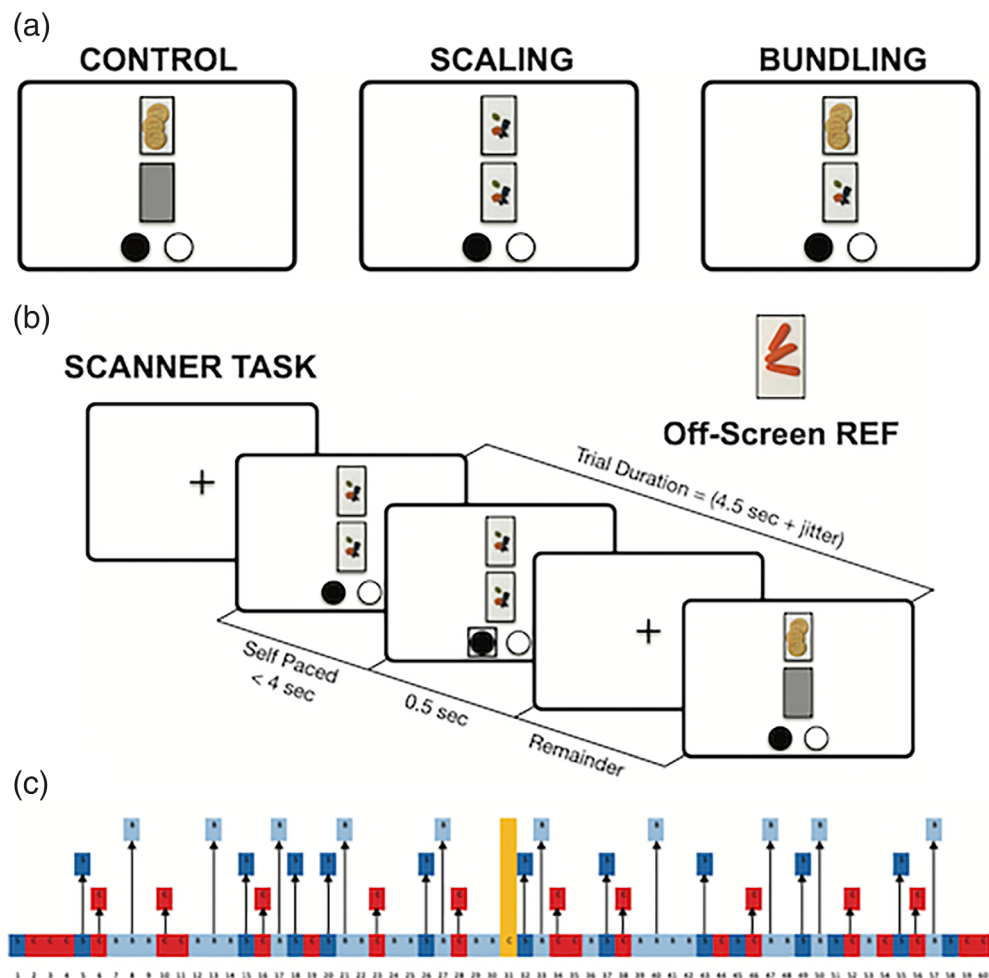

FIGURE 1 Experimental design. (a) Each trial was a choice between the reference item (REF) and a food option in either of three conditions: CONTROL (one single item), SCALING (two same single items) or BUNDLING (two different single items). (b) Only the latter food option was presented on screen. All trials were self-paced. (c) We designed the task to best approximate a distribution of options centered around a REF item (orange) in each task CONTROL (red), SCALING (dark blue), and BUNDLING (light blue). The x-axis represents ranks.

for a total of 90 trials in each condition. Therefore, each participant made 270 choices in the scanner. In each trial, the circles at the bottom of the screen told the participant what button selected which option, the solid circle always representing REF. The button mappings were randomly assigned for each trial.[1] When the participant responded, the circle representing the chosen option was framed in a square to let the participant know that their answer was recorded. The screen then advanced to a fixation cross for the remainder of the trial. The fMRI task was optimized for detecting neural responses. We used Optsec2, a tool that automatically schedules events for rapid presentation event-related fMRI experiments. Trials order and inter-stimulus intervals were optimized for task regressor estimation efficiency (Dale, 1999) and organized into five runs.

We chose the options in order to ensure that each of the three conditions CONTROL, SCALING, and BUNDLING had symmetrical sets of low, medium and high on-screen value options centered around REF. Note that, for a bundle to be less valuable than REF, the latter needed to be more valuable than the single items making the bundle. Therefore, by construction, REF was among the most valuable single items. To separate value specific activity from task specific activity, we also made sure that the distribution of value was similar across conditions. Specifically, for each participant, we used an adapted genetic algorithm that produced three "populations" of options (for CONTROL, SCALING, and BUNDLING) satisfying criteria ensuring similarity across populations in terms of spread of values and distribution around REF (see Figure 1c).

Note that because we wanted to equalize distributions, we did not necessarily end up selecting bundles made of single items that were also selected: many options in the SCALING and BUNDLING conditions contain single items that are not retained for the CONTROL condition, and many single items retained for the CONTROL condition are not part of any option in the SCALING and BUNDLING conditions. This precludes us from studying the aforementioned non linearity effects, or how the value of bundles of scaled items relate to the value of individual items.

2.3 | MRI data acquisition

Neuroimaging data was collected using the 3T Siemens MAGNETOM Tim/Trio scanner at the Dana and David Dornsife Cognitive Neuroscience Imaging Center at USC with a 32-channel head-coil. Participants were laid supine on a scanner bed, viewing stimuli through a mirror mounted on head coil. Blood oxygen level-dependent (BOLD) response was measured by echo planar imaging (EPI) sequence with PACE (prospective acquisition correction) (TR = 2 s; TE = 25 ms; flip angle = 90; resolution = 3 mm isotropic; 64 × 64 matrix in

FOV = 192 mm). A total of 41 axial slices, each 3 mm in thickness were acquired in an ascending interleaved fashion with no interslice gap to cover the whole brain. Slices were acquired on the anterior-posterior-commissure plane (Deichmann et al., 2003). Anatomical images were collected using a T1-weighted three-dimensional magnetization prepared rapid gradient echo (MP-RAGE with TI = 900 ms; TR = 1.95 s; TE: 2260 ms; flip angle = 9; resolution = 1 mm isotropic; 256 × 256 matrix in FOV = 256 mm) primarily for localization and normalization of functional data. These scans were co-registered with the participant's mean EPI images. These images were averaged together to permit anatomical localization of the functional activations at the group level.

2.4 | MRI data preprocessing

Image analysis was performed using Functional Magnetic Resonance Imaging of the Brain (FMRIB) Software Library (FSL) (Jenkinson et al., 2012) algorithms organized in a nipype pipeline. Computation for the work described in this paper was supported by the University of Southern California's Center for High-Performance Computing (hpcc.usc.edu). The structural images were skull-stripped then aligned and spatially normalized to the standard Montreal Neurological Institute (MNI) EPI template. The functional images were motion and time corrected. They were spatially smoothed using a Gaussian Kernel with a full width at half-maximum of 5 mm. We also applied a high-pass temporal filter using a filter width of 120 s.

2.5 | Behavioral analysis

As previously noted, participants were asked to make choices between two snack options. The first option was always the same off-screen reference option denoted by REF while the second option was an on-screen variable option $V AR_j$ ($j = \{1, ..., N\}$). We constructed a Random Utility Model (Clithero & Rangel, 2013a; McFadden, 1973; Train, 2009) in which we assumed that the utility derived by option $V AR_j$ depended on the value of the food snack and a stochastic unobserved error component E_j. Formally, $u(REF) = v_0 + E_0$ and $u(V AR_j) = v_j + E_j$. In this model, the probability of choosing option $V AR_j$ is therefore $P_j = Pr[E_0 - E_j < v_j - v_0]$. Assuming that the error terms are independent and identically distributed and follow an extreme value distribution with cumulate density function $F(E_k) = \exp(-\lambda e^{-Ek})$ for all $k = 0, j$, the probability that the participant chooses option $V AR_j$ is the logistic function:

$$p_j = \frac{1}{1 + e^{-\lambda(v_j - v_0)}}.$$

The model predicts that choices in which values are close yield a 50% chance of choosing one over the other, while choices that are far apart tend to certain outcomes. The model is then used to construct a likelihood function based on the above probabilities and we applied

---

[1] Subjects had button boxes in each hand when they were in the scanner. They were instructed to make choices by pressing a button in the hand corresponding to the option, as represented by the circle, they wanted. For example, if they wanted the reference option and the solid circle was on the right side of the screen in that trial, they could select it by pressing a button in their right hand. If they wanted the on-screen option instead, they could select it by pressing a button corresponding to the hollow circle, which in that case would be a button in their left hand.

Maximum Likelihood Estimation techniques to retrieve parameters v_j given the observed choices for each individual. In practice, this procedure was implemented in Matlab (MathWorks) with standard algorithms, which apply the likelihood function over the entire data, and estimate the value parameters that best match the observed choices. Based on these retrieved values, we assigned implicit rankings across all options (V), and across options in the CONTROL condition (CV), SCALING condition (ScV), and BUNDLING condition (BV).

A few remarks are in order. First, because the value of the reference option is the same across all trials, parameterizing the subjective value of the on-screen option or the subjective value of the difference between the two options (value of on-screen option v_j − value of off-screen reference option v_0) is the same. We can therefore without loss of generality interpret v_j as either the value or the relative value of the on-screen option. Second, the λ model is equivalent to a softmax representation: the probability of choosing an option is a softmax function with temperature $1/\lambda$. This is the case only because the distribution is an extreme value distribution. Third, our model shares features with models that focus on entropy (Bernacer et al., 2019; Goni et al., 2011). This is the case because there is a mathematical connection between entropy and the Random Utility Model (Matějka & McKay, 2015), as there is one between entropy and softmax (which is equivalent to the Boltzmann distribution and maximizes entropy). Last, ideally, we would like to estimate both value parameters and temperature. However, λ is not identified in this simple model (we could rewrite λv_j as V_j and λv_0 as V_0 without affecting the model), making it impossible to estimate both types of parameters at the same time. To estimate subjective value, we normalize λ to 1.

In principle, if a subject's choices are well represented by the Random Utility Model, we should observe that most choices are consistent with estimates and implicit rankings. For each individual, we computed the percentages of choices that were consistent with the value estimates (and henceforth with the implicit rankings) across all conditions and within each condition. We call these percentages *Consistency Rates*. Note that because implicit ranks are only best estimates, a trial that contradicts the ranking and is categorized as inconsistent may not contradict the true underlying preferences (which are not observed). This means that consistency makes sense as an aggregate measure across choices, but it cannot be used to classify individual trials. Note that there is a connection between Consistency Rates and consistency across trials (in a revealed preference argument sense). When a person never reverts their choices, the value estimates reflect no reversals and the choices all agree with the estimates. The estimates reflect how easy/difficult it is to rank an option with respect to the reference option in a way that matches the proportions of reversals. The Consistency Rate aggregates this information across all options. Last, there is also a relationship between the overall Consistency Rate and λ. The Random Utility Model predicts that reversals are more likely when v_j is close to v_0 to an extent modulated by λ. If behavior is consistent with this premise, a low consistency rate is driven by frequent reversals when values are close, which corresponds to a high λ. Said differently, Consistency Rates provide an ex post diagnostic of the uncertainty the person faces to compute subjective values.

2.6 | Analysis of reaction times

We recorded the onset of the stimulus and the time at which a choice was made in each trial. We looked at whether trials deemed to be more difficult, as measured by a smaller distance between the estimated value of the on-screen and off-screen options, were also taking longer. We also looked for systematic differences across conditions and across the type of choices (on screen vs. off-screen). For each participant, we computed the mean *Reaction Time* it took them to deliberate in each of the three conditions. These measures were designed to analyze individual differences across conditions.

2.7 | MRI data analysis

We estimated several general linear models (GLMs) of BOLD responses. Each aspect of the task was encoded in a *regressor* for the GLM. To identify what signal was associated with a particular condition, we constructed *indicator regressors* that take value 1 whenever the participant is performing a trial within a condition and 0 otherwise. To identify the neural activity associated with the subjective value of the on-screen option, we created a *parametric regressor* equal to the value proxy (details below) of the on screen option. The models also included motion parameters (regressors for translation and rotation as well as artifact regressors controlling for quick jerking movements) and regressors for each run as nuisance regressors. All regressors were convolved with the canonical form of the hemodynamic response. The values in the regressors were applied from the onset of the stimulus until a choice was made (average duration, 1.47 s). All of our GLMs took the general form:

$$\text{BOLD}_i = \left[H^1(R^a)\right] * \beta_i{}^a + R^b * \beta_i{}^b + e_i$$

where BOLD_i is the time-series of BOLD signal at each voxel i, H^1 is the hemodynamic response function (HDF) used by FSL applied to the primary regressor matrix R^a (each column is a primary regressor), R^b are regressors of no interest and e_i is a Gaussian noise. The GLM solves for $\beta_i{}^a \beta^a$ and $\beta_i{}^b \beta^b$ to minimize the error e_i. To analyze the influence of an indicator regressor, the coefficients β^a are contrasted against each other. The β^a-contrasts are used to generate interpretable statistics. Every GLM was estimated in several steps. First, we estimated the model separately for each participant. After each GLM was fit to the image time-series, the β-contrasts were combined at the subject level using a Fixed Effects Model, then combined in a Mixed Effects Model to create group level voxel-wise t-statistics converted into z-statistics. All images were thresholded at $z = 3.1$ ($p = .001$). The resulting image was refined further using cluster correction and a significance level of $p < .05$ adjusted for family wise error. Clusters were reported if they passed that threshold unless otherwise noted.

We used FSL Harvard-Oxford Subcortical and Cortical Structural Atlas and Talairach Daemon Labels (https://fsl.fmrib.ox.ac.uk/fsl/fslwiki/Atlases) to list every gray matter region identified within each cluster. Functional regions were added where it was appropriate, using some of the notations from Dixon et al. (2017). For the regions
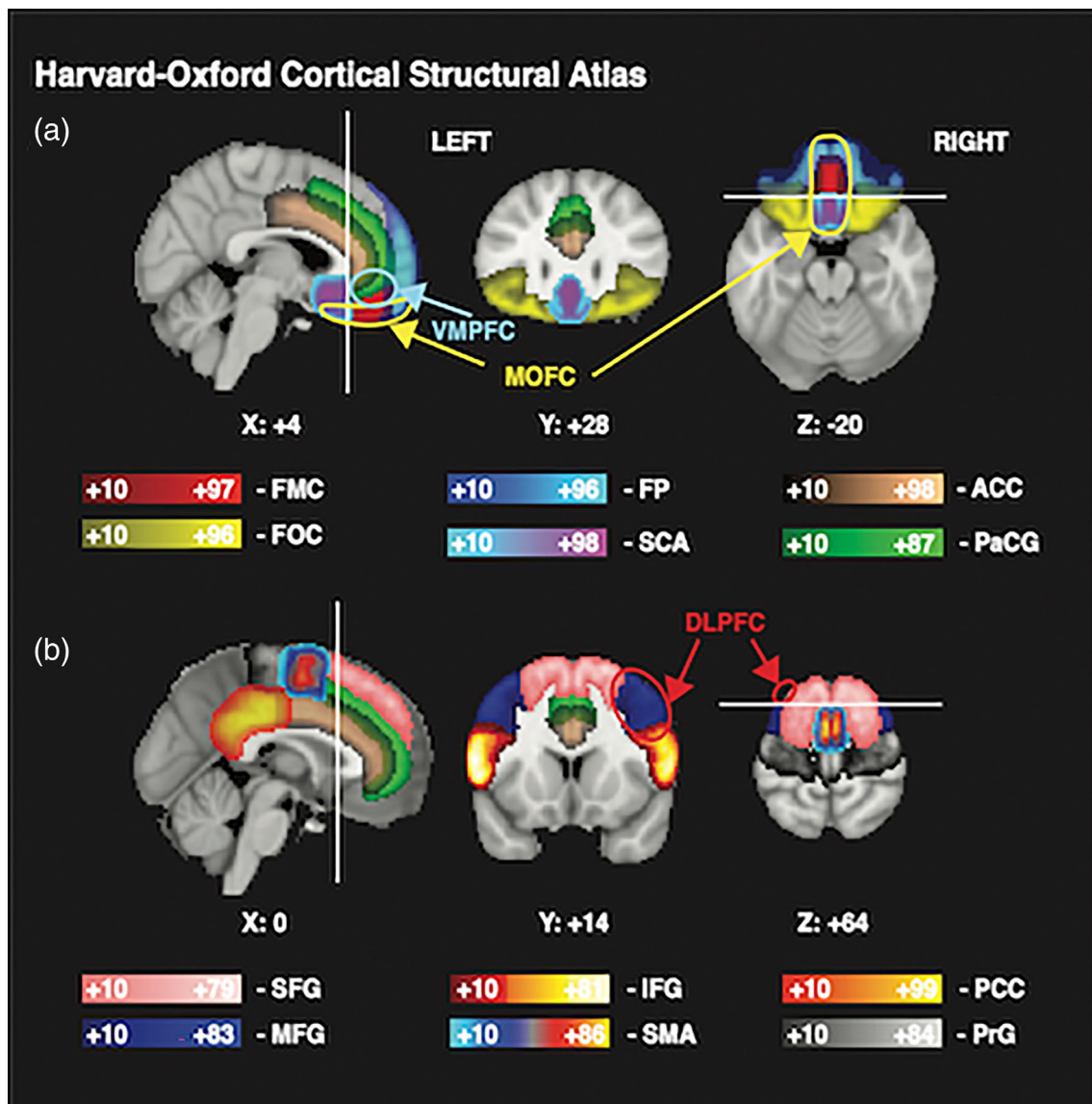
FIGURE 2 Location of VMPFC, MOFC, and DLPFC with regard to Harvard-Oxford cortical structural atlas. (a) Posterior part of VMPFC was defined by the anterior part of subcallosal cortex (at $Y = +28$), while the anterior part of VMPFC was defined by the posterior part of frontal pole (FP), and it overlayed with dorsal part of frontal medial cortex (FMC) and ventral part of paracingulate gyrus/anterior cingulate cortex. MOFC was defined by ventral part of FMC/FP and surrounded by medial parts of frontal orbital cortex. (b) DLPFC was defined according to Dixon et al. (2017) (BA = 9, 46, and 8), by the presence of middle frontal gyrus (as well as junctions with superior frontal gyrus and inferior frontal gyrus), with the most posterior border right before supplementary motor area ($Y = +14$).

for which we formed a priori hypothesis, namely the VMPFC, the MOFC and the DLPFC, and given the ambiguity around their description in the literature, we set an ex ante rule regarding how we would report our evidence (Figure 2).

2.7.1 | Identifying the value tracking regions across all conditions

We used GLM_1 to identify the value tracking region across all conditions. This GLM consisted of four regressors of interest: the (demeaned) implicit ranking value regressor of the on-screen option[2] V and three indicator functions (boxcars) capturing conditions

CONTROL (C), SCALING (Sc), and BUNDLING (B).[3] We report this whole brain analysis in Section 3.2.1. Given the decision-making literature on subjective value has consistently reported certain regions to be significantly associated with value tracking, we were interested in identifying which of these regions overlapped with regions reported elsewhere. For that purpose, we refer to the meta analysis from Clithero and Rangel (2013b) that identifies the set of regions comprising VMPFC and DLPFC among others that consistently track value.

---

[2]Remember that the off screen option is always the same, therefore V can also be interpreted as the difference between the on-screen option and the off-screen option.

[3]Note that, because the off-screen option is always the same, the value regressor is orthogonal to difficulty. BOLD responses that correlates with the value regressor cannot be confounded with BOLD responses that correlate with difficulty.

We call this set *Subjective Value Network*, referred to as "Meta Value" on graphs.[4]

2.7.2 | Testing for differences in value tracking across conditions

We used GLM_2 consisting of the three (demeaned) parametric value regressors CV, ScV, and BV and the three indicator functions C, Sc, and B (boxcars). This GLM allows to test for interaction effects between the value regressor and condition dummies and to analyze differences between conditions within the value tracking region identified by GLM_1 that collapsed all conditions. This whole brain analysis is reported in Section 3.2.2. GLM_2 also allows us to identify the individual condition maps, that is the regions that significantly track value in each condition. We conduct an exploratory analysis of these maps in Section 3.2.3.

2.7.3 | Identifying a common core value tracking system

We ran a second exploratory analysis, a conjunction analysis within GLM_2 to identify which regions track value in all conditions. This analysis retains voxels that are significantly activated (compared with baseline) at the intersection of the individual condition maps. Since inclusion as a finding in this exploratory conjunction contrast required three statistically independent rejections of the null at a given voxel, we used a more liberal $z > 1.645$ ($p < .05$) for this analysis. It is reported in Section 3.2.4.

2.7.4 | Testing for differences in responses to conditions

We used GLM_1 and we computed contrasts of parameter estimates Sc-C, B-C and B-Sc. We identified regions that were differentially activated in each condition compared with the two others by retaining voxels that responded significantly more (less) in CONTROL than SCALING and BUNDLING, significantly more (less) in SCALING than CONTROL and BUNDLING and significantly more (less) in BUNDLING than CONTROL and SCALING. The analysis is reported in Section 3.3.

2.7.5 | Region of interest (ROI) analysis

Given earlier research points to the significant role of the MOFC and the VMPFC in value representation, we had a strong a priori interest in those regions (Hare et al., 2009; Kable & Glimcher, 2007; Plassmann et al., 2007; Sokol-Hessner et al., 2012). The a priori ROI for the VMPFC, hereafter *VMPFC*, was defined by a 10 voxel sphere with the center at [0,46,−6] in MNI152 space. It encompasses VMPFC activity reported in Kahnt et al. (2011), Chib et al. (2009), McClure et al. (2004), O'Doherty et al. (2006), Kim et al. (2010), Lim et al. (2011) and Levy and Glimcher (2011). The a priori MOFC ROI, hereafter *MOFC*, was defined by 7 voxel sphere with the center at [−8,44,−20] in MNI152 space. This corresponds to the area where the "value tracking" activity was reported by Arana et al. (2003). All ROIs were performed on the second level cope images and we extracted each subject's contrast estimates averaged across all of the voxels in the mask. These numbers will be referred to as "mean parameters." We used a significance level of $p < .05$ in statistical tests related to these measures and we applied corrections whenever appropriate. This ROI analysis is reported in Section 3.2.5.

2.7.6 | Studying relationships between neural correlates and choice consistency

To assess whether variations in patterns of activation across individuals predict variations in patterns of behavior, we conducted regression analysis between individual mean parameters in relevant clusters on the one hand and individual consistency rates on the other hand. We retained clusters identified by the analysis of GLM_1 and GLM_2 in the VMPFC and DLPFC. For the contrasts of interest, we extracted each subject's contrast estimates averaged across all of the voxels in the mask from the second level cope images. The clusters and contrasts of interest are further detailed in Section 3.4, where the analysis is reported.

2.7.7 | Other planned analyses

Last, we report in the Supplementary Data S1 a replication that uses the reported ranks elicited before the fMRI session as the value-tracking regressor. This replication adopts the methodology used in many studies and is included for comparison. We also report the results of a planned analysis of difficulty, and a planned connectivity analysis that uses our a priori ROI *VMPFC*.

3 | RESULTS

3.1 | Behavioral measures

3.1.1 | Distribution of options in the pairwise fMRI choice task

As explained earlier, we selected options based on rankings elicited out of the scanner to target an ideal distribution of options (see Figure 1c). However, once in the scanner, bundled options were often more attractive to participants, possibly because hunger had increased from the start of the session, leading to greater relative valuation of

---

[4]Because the off-screen option is always the same, we do not report neural correlates of the chosen option. A proper way of running this analysis requires to remove all the trials in which the off-screen option is chosen to avoid the results to be biased towards that single point. It would therefore amount to run the GLM on the on-screen option value regressor only on the subset of the most valuable items. Because our task is designed such that the off-screen option is chosen 50% of the time, that analysis would have little power.
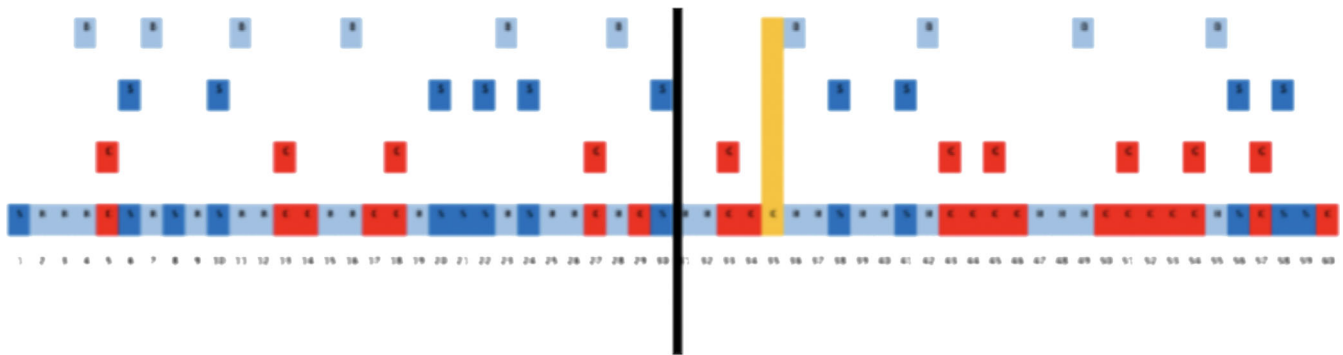
FIGURE 3 Representative realized distribution of on-screen options. On average, options were evenly distributed around REF (orange) in CONTROL (red) but slightly biased towards on-screen options in SCALING (dark blue) and BUNDLING (light blue). For reference, the black mark represents where REF was predicted to be according to the ranking elicited outside the scanner

options with more total calories. On average, options were evenly distributed around REF in CONTROL, there were however 1.93 and 1.73 more options out of 10 to the left of REF (e.g., more valuable than REF) in SCALING and BUNDLING, respectively (see Figure 3). Distributions in SCALING and BUNDLING were otherwise comparable and not excessively different from the distribution of options in CONTROL. As a direct consequence, we observed that 50.7% of trials resulted in choices in favor of the on-screen option in CONTROL, against 60% in SCALING and 61% in BUNDLING.[5]

3.1.2 | Consistency rates

We counted very few missed trials resulting in no choice (1.64% of the trials) indicating that participants were attentive and had enough time to select their preferred option. Also, on average, 90% of the choices of a subject were consistent with their implicit rankings (see Figure 4a), with significant differences only in the comparison between SCALING and BUNDLING ($t = -2.76$, $p = .008$). These rates are consistent with the Economics literature on revealed preferences in young adults. Studies have reported that participants' choices adhere to the existence of well-behaved utility functions and the notion that people have clear rankings of subjective values, resulting in consistency across choices (Andreoni & Miller, 2002; Battalio et al., 1973; Brocas et al., 2019a; Choi et al., 2007; Cox, 1997). Consistency rates also ranged from range 63% to 100%, revealing individual heterogeneity. The spread was relatively small (interquartile range = 0.07, standard deviation = 0.07) and observations below 76% were outliers. They were also correlated across conditions (Pearson's $r = .74$, $p < .001$ between CONTROL and SCALING, Pearson's $r = .69$, $p < .001$ between CONTROL and BUNDLING and Pearson's $r = .80$, $p < .001$ between SCALING and BUNDLING). Last, the proportions of trials that conflicted with the implicit ranks was higher when implicit ranks were close (see Figure 4b). Even though, as explained before, we cannot know whether a specific trial was inconsistent or not (with respect to unobserved true preferences), we can

conclude that more reversals or choices conflicting with each other occurred when options were best fitted as similar. This indicates that such options were more difficult to compare. Note that this is exactly what the Random Utility Model predicts: choices in which values are close yield a 50% chance of choosing one option over the other. From Figure 4b, the chance of choosing the closest options to the right and left of the reference option (smallest non zero difficulty measures) where a bit higher than 50%.

3.1.3 | Reaction times

It took on average longer to make decisions in BUNDLING (mean = 1.62 s) compared with CONTROL (mean = 1.50 s) and SCALING (mean = 1.42 s). A series of paired t-tests and Wilcoxon signed rank tests confirmed that reaction times were significantly longer in BUNDLING compared with CONTROL and SCALING and significantly lower in SCALING compared with CONTROL and BUNDLING (in all cases $p < .001$, see Figure 5a). Reaction times were also correlated across conditions (Pearson's $r = .91$, $p < .001$ between CONTROL and SCALING, Pearson's $r = .90$, $p < .001$ between CONTROL and BUNDLING and Pearson's $r = .894$, $p < .001$ between SCALING and BUNDLING). They were also longer in trials displaying an on-screen option ranked close to REF (see Figure 5b), suggesting that these trials were more difficult and required more deliberation. At the same time, reaction times were shorter when the on-screen option was more appealing than REF (except for very high valued items), suggesting either a salience effect or a tendency to react to more appealing items (Shevlin et al., 2022; Teodorescu et al., 2016). The same was observed by splitting data by condition (not reported). To make sure that the effect was not entirely due to early trials, we also run the analysis by run (not reported). Even though, overall, reaction times decreased, the same distribution was observed. This shows that participants were actively thinking about their choices throughout the experiment, and were not relying on memory of past trials. Last, reaction times were shorter when participants ended up choosing the on-screen option (see Figure 5c). The differences between reaction times when choosing the on-screen option and the off-screen option were similar across conditions.

---

[5]We did not find any relation between individual asymmetries across these distributions and behavioral measures or patterns of brain activity.
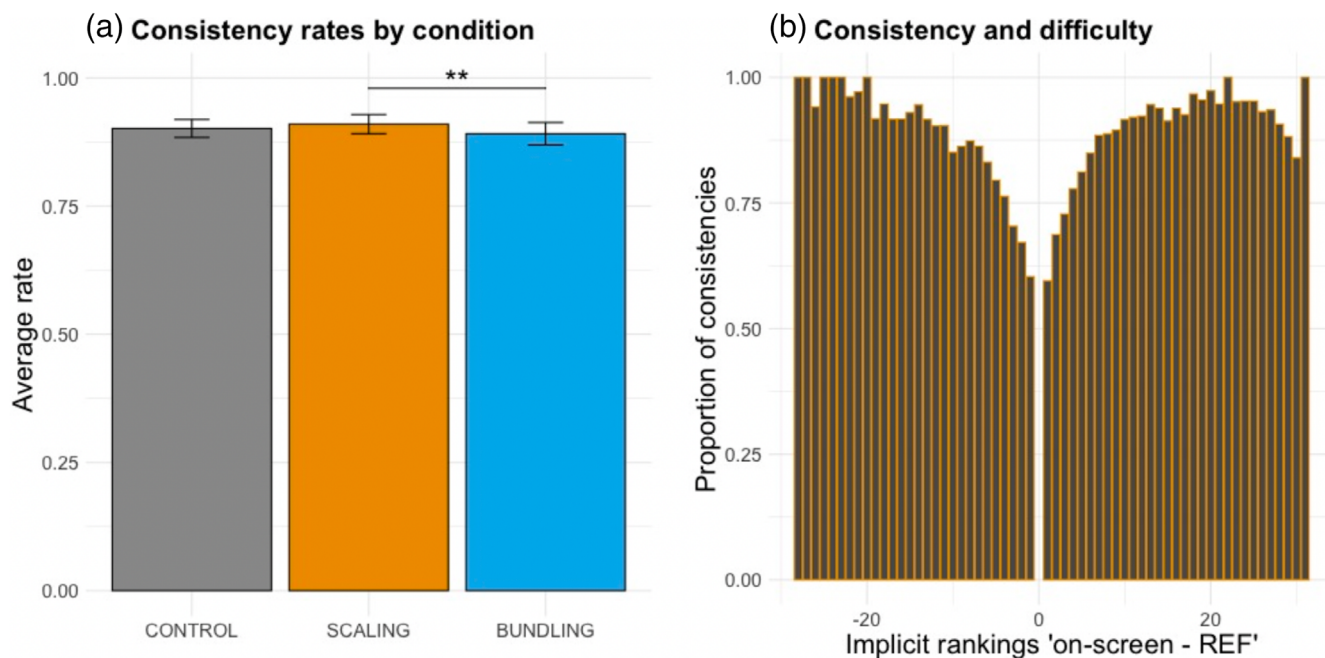
FIGURE 4 Consistency rates. (a) Consistency rates were high and similar across conditions. (b) The proportion of choices conflicting with the best value estimate was higher when choices were similar
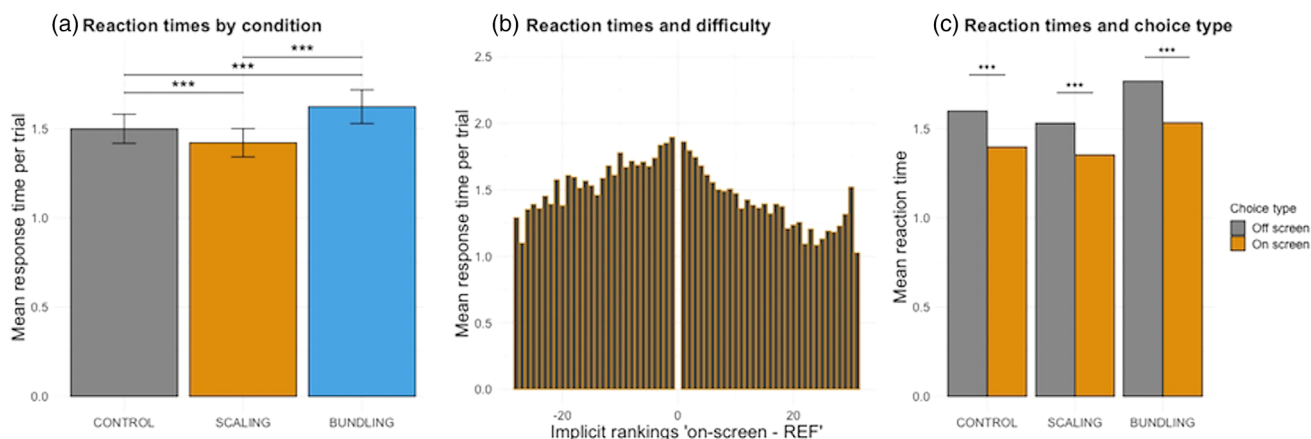

FIGURE 5 Reaction times. (a) It took more time to choose in BUNDLING and less time in SCALING. (b) Mean reaction times as a function of option closeness (difficulty). (c) Mean reaction times as a function of final choice (on-screen or off-screen).

Note that there is also a clear connection between reaction times and consistency rates. Reversals were more frequent on difficult trials, when participants were spending more time.

3.2 | Regions tracking subjective value

3.2.1 | Value tracking regions across conditions

We identified candidates for regions associated with the computation of subjective value by estimating GLM_1. We found that BOLD responses in clusters that overlapped with the *Subjective Value Network* correlated significantly with value (see Figure 6). These included regions overlapping with the VMPFC and the DLPFC. We also found

significant activity in regions not typically associated with value-tracking (e.g., fusiform gyrus and lateral occipital cortex) and usually reported in complex visual processing. We will collectively refer to such regions as *Visual Value*. Last, a signal was also found in the left cerebellum. We report in Table 1 the neural correlates of value during the evaluation period in all trials within the *Subjective Value Network* and outside it, respectively.

3.2.2 | Value tracking differences between conditions

We used GLM_2 to identify differences in value tracking across conditions (Table 2). We found that there was significantly higher activation
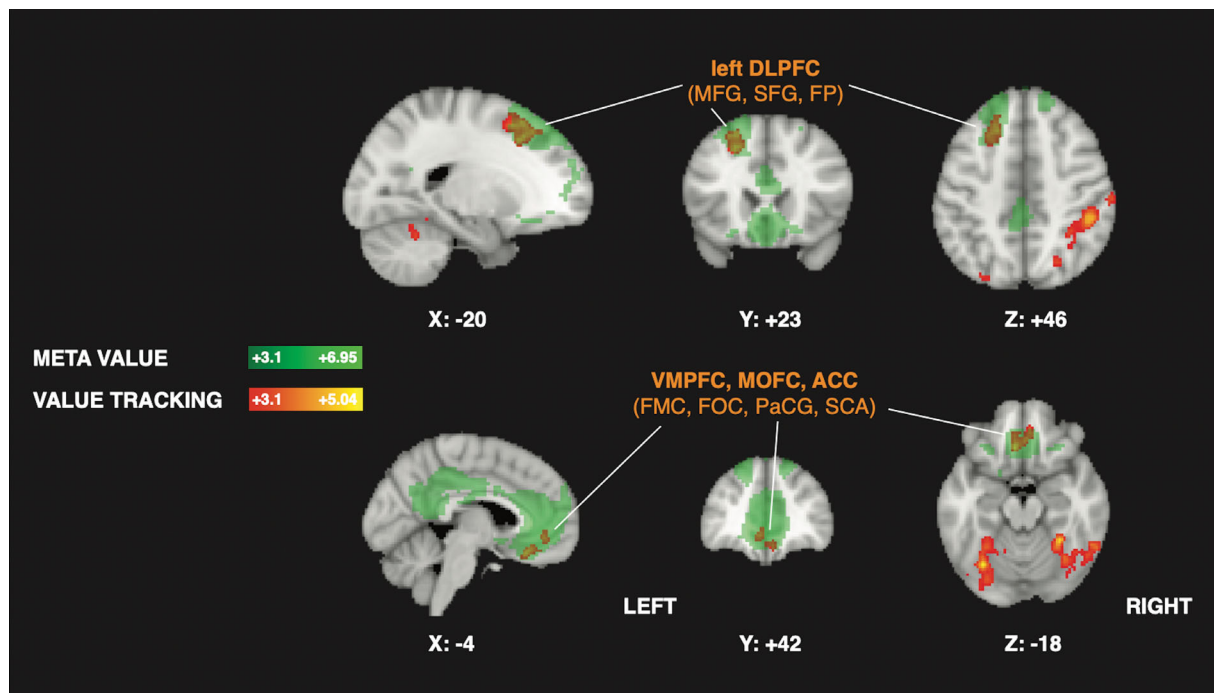
FIGURE 6 Value tracking regions across conditions. Value tracking regions (in red) correlate significantly with *Subjective Value Network* (meta value, in green). Considerable overlap is present in left VMPFC, anterior cingulate cortex, MOFC and left DLPFC.

TABLE 1 Neural correlates of value during the evaluation period across all conditions

Region	k	z-score	x	y	z
(A) Subjective value network					
Left superior frontal gyrus[a]	341	4.44	−22	20	42
Left subcallosal cortex[b]	285	4.41	−6	28	−18
(B) Regions outside the subjective value network					
Right supramarginal gyrus	1381	4.9	48	−38	50
Left occipital fusiform gyrus[c,d]	943	4.95	−32	−66	−18
Right temporal occipital fusiform cortex[c]	855	4.99	28	−48	−16
Left lateral occipital cortex[c]	307	3.89	−30	−78	40

Note: Region is identified as peak activity. Images thresholded at $z = 3.1$ with cluster correction at $p < .05$.
[a]Overlap with DLPFC.
[b]Overlap with VMPFC/MOFC.
[c]Overlap with visual value.
[d]Overlap with left cerebellum.

in CONTROL compared with BUNDLING in regions overlapping with VMPFC/MOFC.

3.2.3 | Value tracking maps in individual conditions

We conducted an exploratory analysis to identify value-tracking regions that were significantly activated in each condition compared with baseline (Table 3). The reader should keep in mind that associations that are significant in one condition but not another do not imply a statistically significant difference in conditions. We found the following patterns: First, in the *Subjective Value Network*, the BOLD response in regions of the VMPFC, the MOFC and the Anterior Cingulate Cortex (ACC) correlated significantly with the value regressor only in the CONTROL condition (Figure 7a). However, the BOLD response in DLPFC was not significantly correlated with the value regressor during any of the three conditions (Figure 7b). Second, there was no significant value tracking activity in the SCALING condition. Last, outside the *Subjective Value Network*, there was significant value tracking activity in CONTROL and BUNDLING. In particular, visual areas (Figure 7c) were significantly tracking value in CONTROL (left Lateral Occipital Cortex) and BUNDLING (Fusiform Gyrus). Last, a cluster located in the Left cerebellum was tracking value in BUNDLING (Figure 7d).

3.2.4 | Common value tracking regions

To identify clusters that responded to value in all conditions, we focused on the map at the intersection of the individual condition maps. Clusters that overlapped with the *Subjective Value Network* were located primarily in the left DLPFC, the left VMPFC and the ACC, and they were located close to the clusters in the VMPFC and the DLPFC that tracked value across conditions. We also found clusters in regions implicated in complex visual processing and the Left Cerebellum. Table 4 summarizes the clusters of relevance within the core value region.

3.2.5 | Value-tracking activity in a priori regions of interest

We performed an analysis of our two independent ROI, *VMPFC*, and *MOFC* (Figure 8). In both cases, mean parameters were significantly different from 0 across conditions ($t = 3.32$; $p = .002$ and $t = 3.12$; $p = .003$, respectively). Analysis of variance did not reveal any difference across conditions (One-way analysis of means, $f = 2.43$, $p = .091$ and $f = 2.82$, $p = .062$) and pairwise t-tests did not identify single differences either (all FDR adjusted $p > .12$ and $>.07$, respectively).

TABLE 2 Differences in value tracking response across conditions

Regions	k	z-score	x	y	z
CV > BV					
Ventromedial prefrontal cortex[a]	108	3.78	2	58	−16

Note: Images thresholded at $z = 3.1$ with cluster correction at $p < .05$.
[a]Overlap with VMPFC/MOFC.

3.2.6 | Value-tracking summary

The findings reveal similarities and differences in activation patterns across conditions. Regions comprising clusters in (i) the left VMPFC and the left DLPFC, (ii) the visual cortex, and (iii) the left cerebellum track value within and across all conditions. Significant differences across conditions have been found in VMPFC regions that show higher activation in CONTROL compared with BUNDLING. While no other differences are detected with conservative thresholds, exploratory analyses suggest that the individual condition maps (where activation is significant with respect to baseline, given conservative thresholds) may differ. There is in particular no significant activity (compared with baseline) in the SCALING condition.

3.3 | Main effect of condition on neural activity

The study of condition regressors in GLM_1 reveals that BOLD activity in regions in the left DLPFC, including clusters at the junction with the left VLPFC and regions in the right DLPFC including clusters at the junction with the right VLPFC, was significantly higher in CONTROL and BUNDLING (Figure 9a). Also, BOLD activity in clusters located in the Left/Right cerebellum was higher in BUNDLING (Figure 9b).

3.4 | Neural correlates of choice consistency

In this section, we ask whether individual variations in choice consistency are associated with individual variations in patterns of activity in the VMPFC and the DLPFC. The VMPFC has been associated with the ability to make consistent choices in a lesion study (Camille et al., 2011). The DLPFC is involved in working memory, which itself has been associated with consistency (Brocas et al., 2019a). We retain

TABLE 3 Neural correlates of value during the evaluation period within conditions

Region	k	z-score	x	y	z
(A) CV: Regions responding significantly to CV					
Right temporal occipital fusiform cortex[a]	782	5.06	48	−56	−24
Left lateral occipital cortex[a]	773	5.00	−50	−74	−10
Left subcallosal cortex[b,c]	760	4.52	−6	30	−18
Left lateral occipital cortex	341	4.32	−30	−76	40
Right posterior cingulate cortex[b]	302	4.02	6	−52	20
(B) ScV: Regions responding significantly to ScV					
None					
(C) BV: Regions responding significantly to BV					
Right precentral gyrus	712	4.29	36	−10	62
Left temporal occipital fusiform cortex[a,d]	373	5.41	−28	−44	−22
Right occipital fusiform gyrus[a]	207	4.25	40	−64	−14

Note: Region is identified as peak activity. Images thresholded at $z = 3.1$ with cluster correction at $p < .05$.
[a]Overlap with visual value.
[b]Overlap with subjective value network.
[c]Overlap with VMPFC/MOFC.
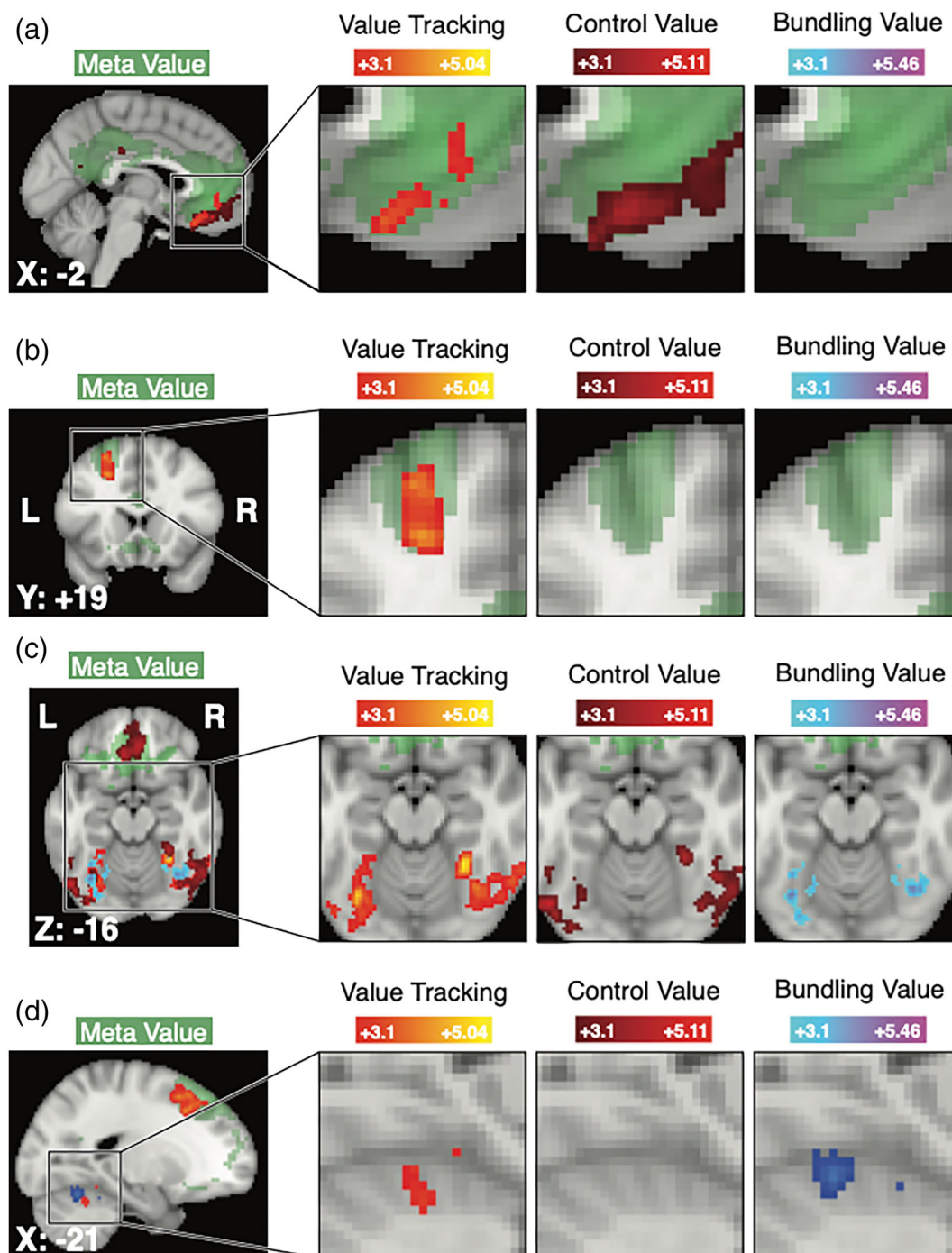[d]Overlap with left cerebellum.

FIGURE 7 Value tracking maps. (a) The VMPFC tracks value across conditions (orange) and in CONTROL (red); (b) The left DLPFC tracks value across conditions only; (c) Regions involved in visual processing track value across conditions and specifically in CONTROL and BUNDLING (blue); (d) clusters in the Left cerebellum track value across condition and in BUNDLING. (Subjective Value Network (green) represented for reference).

four clusters that demonstrate higher responses to increases in value (compared with baseline) in our study. The first two are extracted from GLM1 and reported in Table 1: *VMPFC-1* corresponds to the cluster that overlaps with VMPFC; *DLPFC-1* corresponds to the cluster that overlaps with DLPFC. These regions respond to increase in value across all conditions. The last two are extracted from the conjunction of the individual condition maps and are reported in Table 4: *VMPFC-2* corresponds to the cluster that overlaps with VMPFC; *DLPFC-2* corresponds to the cluster that overlaps with DLPFC. These regions respond to increases in value in all individual conditions. Dependent variables are individual mean parameters in the clusters of interest. Independent variables are individual

TABLE 4 Neural correlates of value common to all conditions within and outside of the Subjective Value Network

Region	k	x	y	z
(A) Subjective value network				
Left dorsolateral prefrontal cortex[a]	287	−24	12	42
Left ventromedial prefrontal cortex[b]	49	−6	30	−16
Right superior frontal gyrus	44	6	38	30
Right frontal pole	20	12	60	18
Right anterior cingulate cortex	8	6	30	10
	7	12	40	−2
	2	6	2	26
Anterior cingulate cortex	3	4	−2	30
Left anterior cingulate cortex	1	−6	40	4
(B) Regions outside the Subjective Value Network				
Right temporal occipital fusiform gyrus[c]	82	40	−48	−24
Left lateral occipital cortex[c]	60	−26	−54	−24
Left cerebellum[d]	6	−22	−54	−26

Note: Images thresholded at *z* < 1.645, uncorrected.
[a]Overlap with DLPFC.
[b]Overlap with VMPFC/MOFC.
[c]Overlap with visual value.
[d]Overlap with left cerebellum.

TABLE 5 Divergent processing in DLPFC/VLPFC and cerebellum

Region	k	x	y	z
Control > scaling & bundling				
Left dorsolateral prefrontal cortex	391	−24	16	36
Left dorso- and ventro-lateral prefrontal cortex	60	−54	2	28
Scaling < control & bundling				
Right dorso- and ventro-lateral prefrontal cortex	554	44	16	14
Left dorso- and ventro-lateral prefrontal cortex	245	−36	8	18
Bundling > control & scaling				
Left/right cerebellum	35	4	−78	−30

Note: Images thresholded at *z* = 3.1 with cluster correction at *p* < .05.

consistency rate and condition dummy variables used as controls. We use robust standard errors (Table 6). Higher mean parameters in both DLPFC regions were associated with higher consistency scores. We also found a positive association between consistency scores and mean parameters in the common VMPFC region.

4 | DISCUSSION

We hypothesized that value representation was modulated by the specific way options are bundled when presented to a decision-maker. We categorized choices between single items as simple and choices involving two single items as complex. In line with the hypothesis, we expected to see different neural patterns within known value-tracking regions, such as the VMPFC and the MOFC. We also expected that more complex options, such as bundles made of heterogenous items,

would be associated with more activity in regions implicated in cognitive processes including working memory. Therefore, we hypothesized that clusters in the DLPFC would be differentially activated especially in the BUNDLING condition. We asked four questions: (1) Is there a common value tracking region when options are simple and complex? (2) What are the neural correlates of value as a function of complexity? (3) Does valuation of multiple goods recruit networks implicated in attention and working memory? and (4) Do consistent choices across conditions have a neural signature? Our findings suggest that there is a common value region comprising the VMPFC and the DLPFC, however additional regions are identified as tracking value, sometimes as a function of task demands. First, regions involved in high-order visual processing were associated with value-tracking. Second, clusters in the left and right DLPFC at the junction of the VLPFC responded differently to conditions, revealing divergent processing across conditions. Last, we observed unexpected patterns
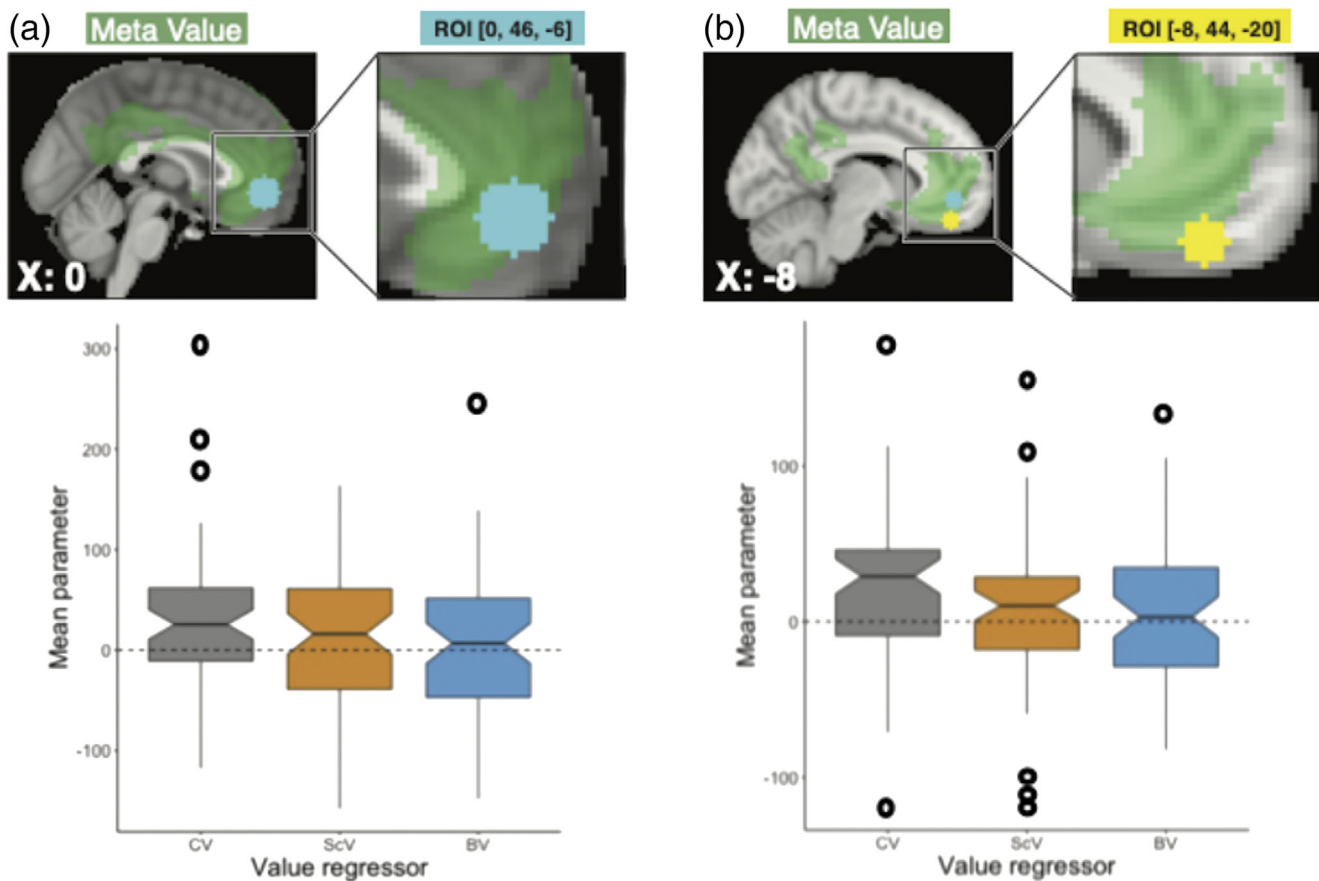
FIGURE 8 Value tracking activity in a priori regions of interest. (a) Distribution of mean parameters in *VMPFC* across conditions and (b) distribution of mean parameters in *MOFC* across conditions.

of activation in clusters located in the cerebellum: BOLD responses in voxels in the right/left cerebellum were significantly higher in the BUNDLING condition, and voxels in the left cerebellum tracked value. However, the results did not support our ex ante categorization of choices: decisions in SCALING took less time and exhibited less neural activity in critical regions. We also did not find that DLPFC was more critically involved in the more complex BUNDLING condition. Still, activity in clusters of the DLPFC was in line with the possibility that DLPFC supports consistency of decisions across trials and across conditions.

We found significant differences in value-tracking patterns only in the VMPFC/MOFC: this region was differentially activated in CONTROL compared with BUNDLING. Our exploratory analysis also revealed that the individual condition maps associated with value tracking did not look alike. We found strong support for the involvement of the VMPFC in the condition closest to earlier experimental settings (Konovalov & Krajbich, 2019) but less for the valuation of scaled and bundled options. In particular, there was no significant activity (compared with baseline) during the evaluation period in SCALING and BUNDLING after cluster correction. This result is consistent with studies that did not observe value-related activity in the VMPFC (de Berker et al., 2019; Hunt et al., 2013; Jocham et al., 2014). Still, using a more liberal threshold and restricting to voxels that were tracking value in all tasks, we found that a cluster

located in the VMPFC belonged to this map. Clusters in the left DLPFC also tracked value in our study. While the effect was small and not always detected after appropriate whole-brain corrections, a cluster in the DLPFC was also present in the intersection map that retains voxels active in all tasks. Given any set of EPI acquisition parameters, signal loss due to susceptibility artifact varies as a function of Z-plane orientation (Weiskopf et al., 2006). In the present study, slice acquisition was standardized to the AC-PC line, which does not optimize sensitivity within the VMPFC. Although not without trade-off (especially lowered sensitivity in the temporal poles) a negative acquisition tilt may have improved our power to test hypotheses related to VMPFC activity.

Value-tracking recruited regions involved in visual processing (fusiform gyrus, lateral occipital cortex). It has been shown in other studies that higher value targets are associated with greater visual activation (Anderson et al., 2014; Serences, 2008; Serences & Saproo, 2010; Tang et al., 2012). It has also been shown that activity in the fusiform gyrus correlates with the aesthetic of visual attributes and exhibits functional connectivity with VMPFC area involved in value computation (Lim et al., 2013), a coupling we also observe in our setting (see Supplementary Data S1).

Some regions in the DLPFC and VLPFC were differentially associated with conditions. Different patterns of activity in these regions may be used to detect the characteristics of the on-screen option and
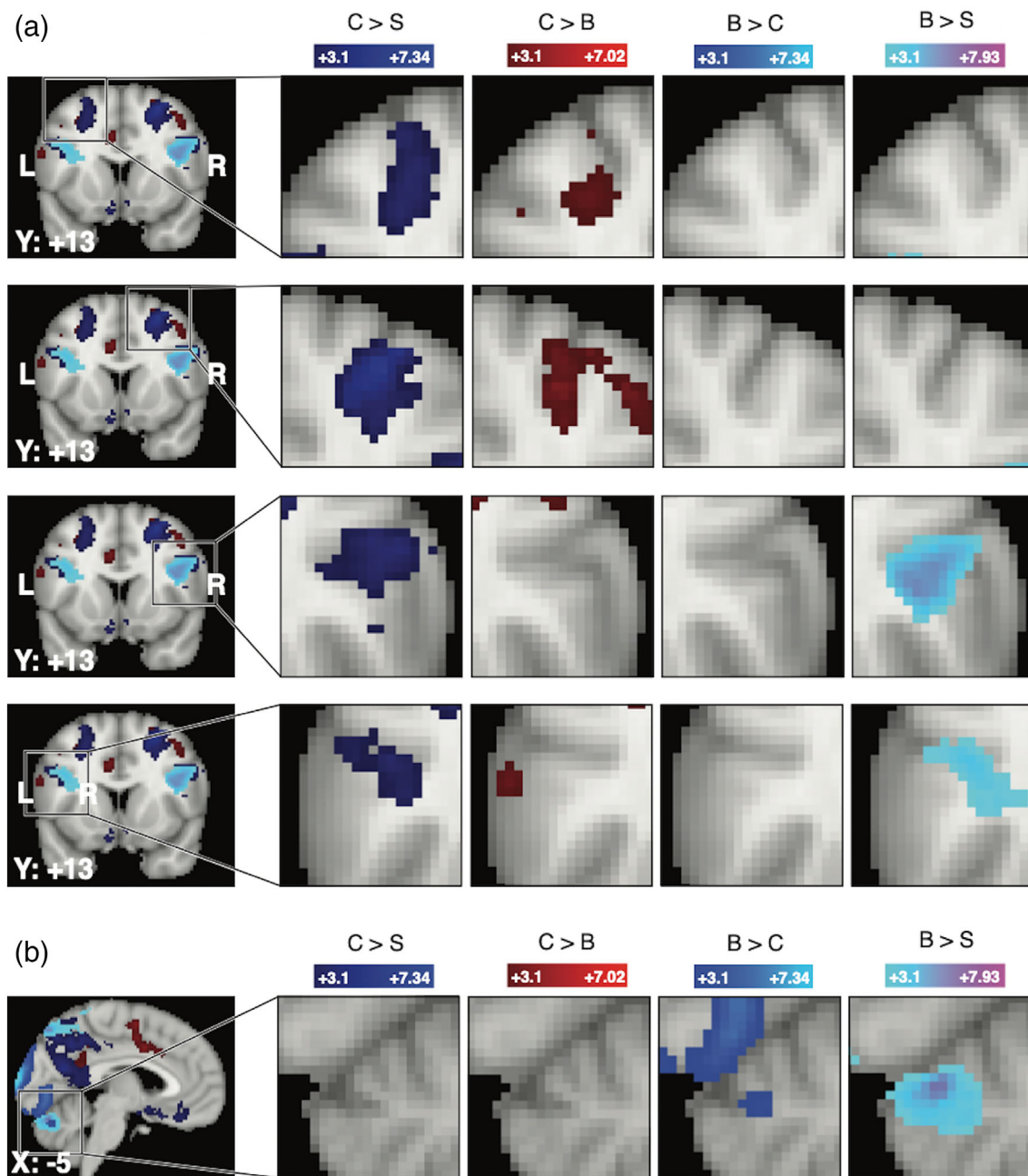
FIGURE 9 Differences in responses to condition. (a) Several clusters in the DLPFC and at the junction of the VLPFC responded differentially to conditions; (b) Several clusters in the left/right cerebellum exhibited differential activity in BUNDLING compared with CONTROL and SCALING (heat-maps represent z-values). Within these regions, several clusters were uniquely associated with conditions (Table 5). First, there was divergent processing between single items and bundles resulting in higher activity in two clusters in the left DLPFC and the left VLPFC in CONTROL. Second, there was also divergent processing between SCALING versus CONTROL and BUNDLING conditions, resulting in lower activity in two clusters in the left and right DLPFC, at the junction of the VLPFC in SCALING. Last, BUNDLING recruited a subset of voxels in the left/right cerebellum, where BOLD activity was systematically higher in that condition. We also checked that differences in activation across conditions in those clusters were not correlated with differences in reaction times, suggesting that higher activation was not mechanically induced by higher evaluation times (PCCs ranging from 0.12 to 0.3 with p values < .05)

help recruit the task-relevant value-tracking regions. This latter conjecture is in line with the role of the VLPFC in response inhibition and goal appropriate response selection (Aron et al., 2004), as well as its role in the integration of choice characteristics to represent subjective value (Fujiwara et al., 2018). An alternative block design that groups trials of the same condition together would help disentangle between the two possible conjectures.

We unexpectedly found that clusters located around the cerebellum were tracking value and were activated differentially across conditions. Even though, the connection between decision-making and

TABLE 6 Relationship between ROI mean parameters and choice consistency

	VMPFC-1	DLPFC-1	VMPFC-2	DLPFC-2
Consistency rate	44.940	66.801**	91.52*	68.56**
	(36.104)	(32.653)	(53.07)	(32.45)
Scaling	−9.926	1.252	−13.27	−9.05
	(9.742)	(5.766)	(11.62)	(6.07)
Bundling	−22.828	2.601	−15.79	−7.37
	(9.588)	(7.733)	(13.18)	(7.24)
Constant	−19.968	−53.945*	−52.91	−41.64
	(33.783)	(30.079)	(47.06)	(28.49)
Observations	60	60	60	60
Mult. R^2	0.038	0.018	0.022	0.028

Note: Of the overall value-tracking regions, only DLPFC was associated with consistency. Of the common value-tracking regions, both VMPFC and DLPFC were associated with consistency. *$p < .1$, **$p < .05$, ***$p < .01$, ****$p < .001$. Robust (clustered) standard errors at the subject level.

cerebellar functions remains unclear, the finding is reminiscent of other studies (in other domains) that revealed a role for the cerebellum in decision-making. Cerebellar circuitry has been associated with computations that support accurate performance in perceptual decision-making tasks (Deverett et al., 2018) and high-level functions (Cardoso et al., 2014; Rosenbloom et al., 2012). Lesion studies have shown that patients with cerebellar damage perform worse than control groups in tasks such as the Stroop Test (Gottwald et al., 2004), the Wisconsin Card Sorting Task (Karatekin et al., 2000) and in instruments that assess cognitive flexibility (Manes et al., 2009). The cerebellum has also been linked more directly to the maintenance of working memory (Deverett et al., 2019; Grimaldi & Manto, 2012). These associations are likely promoted by reciprocal connections between the cerebellum and the prefrontal cortex (present in both human and non-human primates) (Rosenbloom et al., 2012). Moreover, it has also been shown that the right cerebellar hemisphere is associated with logical reasoning while the left cerebellum mediates attentional and visuo-spatial skills (Baillieux et al., 2010). These latter skills might be more relevant in the BUNDLING context, resulting in a condition specific response. Also, activity in the cerebellum may be due to its motor-related function. Indeed, it is possible that highly attractive options may have caused participants to press the button more strongly, resulting in associations with value tracking.

The results obtained in the SCALING condition were the most unexpected. Even though, the on-screen option was a priori more complex to evaluate than a single item, it took less time compared with the two other conditions. At the same time, signal increase within regions relevant in decision making was generally lower during this task condition relative to the CONTROL condition. These two related anomalies are puzzling, but the analysis allows us to rule out certain explanations. Even though participants made choices slightly different from what they were expected (given their rankings outside the scanner), the bias was small and not different across the SCALING and BUNDLING conditions. The results were therefore not due to design or calibration issues applying to the SCALING condition differentially. We also did not find more choice inconsistencies and the

value regressor captured choices equally well. There was also no difference regarding how participants dealt with trials ending in an onscreen choice versus an off-screen choice across conditions. Overall, choice measures did not indicate that the processing of value was different, only reaction times and neural data did. Another possible explanation relies on the fact that choices were self-paced and generated differences in reaction times, which may have artificially produced higher activation in CONTROL and BUNDLING compared with SCALING as sometimes reported in the literature (Grinband et al., 2008; Poldrack, 2015). However, we found that differences in reaction times were not associated with differences in signals, indicating that spending more time on the task did not result in higher activation in a given condition compared with another.

The anomalies in the SCALING condition hinted to the possibility that participants used a "heuristic", a rule such that a participant comes to decide to make decisions on the basis of amount alone, without integrating the taste attribute. Said differently, value computation may have been complemented by a parallel non value-based process to which a participant switch when efficient. Heuristic usage has already been suggested as an explanation of behavior in value-based decision-making paradigms (Brocas et al., 2019a, 2019b). A "more is better" rule may have been applied in our context. Because the choices in the scanner were globally consistent with the rankings provided outside the scanner, it is likely that the same processes were used in both cases. This suggests that it is not an artifact of the experimental task, but a naturally occurring process worth investigating further. A first step would be to contrast the results with a task in which REF is also a scaled option. There was also a small change in reaction times over the course of the experiment, suggesting that participants may have started valuing quantity more as they became hungrier, adopting a behavior that looks like a heuristic while it only reflects a change in priorities. Alternatively, a decrease in reaction times may be explained by a differential accumulation of information that uses characteristics of the task to efficiently save on costs of processing. For instance, a model in which the brain keeps track of twice the current accumulated value may help reach a decision threshold sooner. It is

unclear however how this model should be extended to heterogenous bundles which also feature externalities between items (e.g., consuming a sweet and a salty snack in two different events is different from consuming them together). More studies of the valuation process in the presence of quantities, in particular studies where one could compare the value of single items and the value of their respective bundles, are needed to understand why value is computed differentially in SCALING and BUNDLING.

Even though, we observed little variance in consistency measures across individuals, which is to be expected in a population of undergraduate students (Brocas et al., 2019a), we found that differences in activity patterns in both the VMPFC and the DLPFC were explained by variations in individual consistency rates. We conjecture that consistency results from a reduction in noise around the trial-by-trial valuation process, rather than an ability to remember past choices and repeat them. The latter has been reported only in participants (faculty and PhD students) with familiarity with revealed preference theory who were concerned with avoiding embarrassing violations of rationality (Harbaugh et al., 2001). Participants are otherwise not believed to track their choices to buy consistency in revealed preferences tasks. The fact that the distributions of reaction times as a function of difficulty were the same across runs supports the hypothesis that participants were actively considering their choices. The noise-reduction mechanism responsible for consistency may be supported by the DLPFC. Indeed, the involvement of the VMPFC in choice consistency has already been documented in Camille et al. (2011) in a lesion study. An impairment of the VMPFC has a direct effect on the ability to evaluate options. Our study suggests the possibility that DLPFC is required to keep the valuation process consistent, even when VMPFC is not impaired. Said differently, VMPFC and DLPFC may work jointly to provide an accurate representation of value in each trial, resulting in consistent choices across trials.

AUTHOR CONTRIBUTIONS

Jekaterina Zyuzin: investigation, formal analysis, data curation, writing; Dalton Combs: conceptualization, methodology, software; John Monterosso: conceptualization, methodology, supervision, reviewing and editing, funding acquisition; Isabelle Brocas: conceptualization, methodology, formal analysis, supervision, project administration, resources, writing, reviewing and editing, funding acquisition.

ACKNOWLEDGMENTS

DATA AVAILABILITY STATEMENT

The datasets generated for this study will be made publicly available upon publication. The same will apply to the main codes that contributed to run both the behavioral and neuro-imaging analyses.

ORCID

Isabelle Brocas https://orcid.org/0000-0001-5847-1428

REFERENCES

Anderson, B. A., Laurent, P. A., & Yantis, S. (2014). Value-driven attentional priority signals in human basal ganglia and visual cortex. *Brain Research*, *1587*, 88–96.

Andreoni, J., & Miller, J. (2002). Giving according to garp: An experimental test of the consistency of preferences for altruism. *Econometrica*, *70*(2), 737–753.

Arana, F. S., Parkinson, J. A., Hinton, E., Holland, A. J., Owen, A. M., & Roberts, A. C. (2003). Dissociable contributions of the human amygdala and orbitofrontal cortex to incentive motivation and goal selection. *Journal of Neuroscience*, *23*(29), 9632–9638.

Aron, A. R., Robbins, T. W., & Poldrack, R. A. (2004). Inhibition and the right inferior frontal cortex. *Trends in Cognitive Sciences*, *8*(4), 170–177.

Baillieux, H., de Smet, H. J., Dobbeleir, A., Paquier, P. F., de Deyn, P. P., & Marien, P. (2010). Cognitive and affective disturbances following focal cerebellar damage in adults: A neuropsychological and spect study. *Cortex*, *46*(7), 869–879.

Baker, S. C., Frith, C. D., Frackowiak, S. J., & Dolan, R. J. (1996). Active representation of shape and spatial location in man. *Cerebral Cortex*, *6*(4), 612–619.

Bartra, O., McGuire, J. T., & Kable, J. W. (2013). The valuation system: A coordinate-based meta-analysis of bold fMRI experiments examining neural correlates of subjective value. *NeuroImage*, *76*, 412–427.

Battalio, R. C., Kagel, J. H., Winkler, R. C., Fisher, E. B., Basmann, R. L., & Krasner, L. (1973). A test of consumer demand theory using observations of individual consumer purchases. *Economic Inquiry*, *11*(4), 411–428.

Baumgartner, T., Knoch, D., Hotz, P., Eisenegger, C., & Fehr, E. (2011). Dorsolateral and ventromedial prefrontal cortex orchestrate normative choice. *Nature Neuroscience*, *14*(11), 1468–1474.

Berman, K. F., Ostrem, J. L., Randolph, C., Gold, J., Gold-Berg, T. E., Coppola, R., Carson, R. E., Herscovitch, P., & Weinberger, D. R. (1995). Physiological activation of a cortical network during performance of the Wisconsin card sorting test: A positron emission tomography study. *Neuropsychologia*, *33*(8), 1027–1046.

Bernacer, J., Martinez-Valbuena, I., Martinez, M., Pujol, N., Luis, E., Ramirez-Castillo, D., & Pastor, M. A. (2019). Neural correlates of effort-based behavioral inconsistency. *Cortex*, *113*, 96–110.

Braver, T. S., Cohen, J. D., Nystrom, L. E., Jonides, J., Smith, E. E., & Noll, D. C. (1997). A parametric study of prefrontal cortex involvement in human working memory. *NeuroImage*, *5*(1), 49–62.

Brocas, I., & Carrillo, J. D. (2021). Value computation and modulation: A neuroeconomic theory of self-control as constrained optimization. *Journal of Economic Theory*, *198*, 105366.

Brocas, I., Carrillo, J. D., Dalton Combs, T., & Kodaverdian, N. (2019a). Consistency in simple vs. complex choices by younger and older adults. *Journal of Economic Behavior & Organization*, *157*, 580–601.

Brocas, I., Carrillo, J. D., Dalton Combs, T., & Kodaverdian, N. (2019b). The development of consistent decision-making across economic domains. *Games and Economic Behavior*, *116*, 217–240.

Brooks, S. J., Daly, O. G. O., Uher, R., Friederich, H.-C., Giampietro, V., Brammer, M., Williams, S. C. R., Schioth, H. B., Treasure, J., & Campbell, I. C. (2011). Differential neural responses to food images in women with bulimia versus anorexia nervosa. *PLoS One*, *6*(7), e22259.

Camille, N., Griffiths, C. A., Vo, K., Fellows, L. K., & Kable, J. W. (2011). Ventromedial frontal lobe damage disrupts value maximization in humans. *Journal of Neuroscience*, 31(20), 7527–7532.

Camus, M., Halelamien, N., Plassmann, H., Shimojo, S., O'Doherty, J., Camerer, C., & Rangel, A. (2009). Repetitive transcranial magnetic stimulation over the right dorsolateral prefrontal cortex decreases valuations during food choices. *European Journal of Neuroscience*, 30(10), 1980–1988.

Carlson, S., Martinkauppi, S., Rama, P., Salli, E., Korvenoja, A., & Aronen, H. J. (1998). Distribution of cortical activation during visuospatial n-back tasks as revealed by functional magnetic resonance imaging. *Cerebral Cortex (New York, NY: 1991)*, 8(8), 743–752.

Chen, F., He, Q., Han, Y., Zhang, Y., & Gao, X. (2018). Increased bold signals in dlPFC is associated with stronger self-control in food-related decision-making. *Frontiers in Psychiatry*, 9, 689.

Chib, V. S., Rangel, A., Shimojo, S., & O'Doherty, J. P. (2009). Evidence for a common representation of decision values for dissimilar goods in human ventromedial prefrontal cortex. *Journal of Neuroscience*, 29(39), 12315–12320.

Choi, S., Fisman, R., Gale, D., & Kariv, S. (2007). Consistency and heterogeneity of individual behavior under uncertainty. *American Economic Review*, 97(5), 1921–1938.

Christoff, K., Prabhakaran, V., Dorfman, J., Zhao, Z., Kroger, J. K., Holyoak, K. J., & Gabrieli, J. D. E. (2001). Rostrolateral prefrontal cortex involvement in relational integration during reasoning. *NeuroImage*, 14(5), 1136–1149.

Clithero, J. A., & Rangel, A. (2013a). *Combining response times and choice data using a neuroeconomic model of the decision process improves out-of-sample predictions*. California Institute of Technology unpublished.

Clithero, J. A., & Rangel, A. (2013b). Informatic parcellation of the network involved in the computation of subjective value. *Social Cognitive and Affective Neuroscience*, 9(9), 1289–1302.

Cohen, J. D., Forman, S. D., Braver, T. S., Casey, B. J., Servan-Schreiber, D., & Noll, D. C. (1994). Activation of the prefrontal cortex in a nonspatial working memory task with functional mri. *Human Brain Mapping*, 1(4), 293–304.

Cohen, J. D., Perlstein, W. M., Braver, T. S., Nystrom, L. E., Noll, D. C., Jonides, J., & Smith, E. E. (1997). Temporal dynamics of brain activation during a working memory task. *Nature*, 386(6625), 604.

Cox, J. C. (1997). On testing the utility hypothesis. *The Economic Journal*, 107(443), 1054–1078.

Dale, A. M. (1999). Optimal experimental design for event-related FMRI. *Human Brain Mapping*, 8(2–3), 109–114.

Dalton, B., Foerde, K., Bartholdy, S., McClelland, J., Kekic, M., Grycuk, L., Campbell, I. C., Schmidt, U., & Steinglass, J. E. (2020). The effect of repetitive transcranial magnetic stimulation on food choice-related self-control in patients with severe, enduring anorexia nervosa. *International Journal of Eating Disorders*, 53(8), 1326–1336.

de Berker, A. O., Kurth-Nelson, Z., Rutledge, R. B., Bestmann, S., & Dolan, R. J. (2019). Computing value from quality and quantity in human decision-making. *Journal of Neuroscience*, 39(1), 163–176.

Deichmann, R., Gottfried, J. A., Hutton, C., & Turner, R. (2003). Optimized EPI for fMRI studies of the orbitofrontal cortex. *Neuroimage*, 19(2), 430–441.

Cardoso, C. O., Branco, L. D., Cotrena, C., Kristensen, C. H., Di Giorge, D., Bakos, S., & Fonseca, R. P. (2014). The impact of frontal and cerebellar lesions on decision making: Evidence from the Iowa gambling task. *Frontiers in Neuroscience*, 8, 61.

de Wit, S., Corlett, P. R., Aitken, M. R., Dickinson, A., & Fletcher, P. C. (2009). Differential engagement of the ventromedial prefrontal cortex by goal-directed and habitual behavior toward food pictures in humans. *Journal of Neuroscience*, 29(36), 11330–11338.

Demb, J. B., Desmond, J. E., Wagner, A. D., Vaidya, C. J., Glover, G. H., & Gabrieli, J. D. (1995). Semantic encoding and retrieval in the left inferior prefrontal cortex: A functional MRI study of task difficulty and process specificity. *Journal of Neuroscience*, 15(9), 5870–5878.

Deverett, B., Kislin, M., Tank, D. W., Samuel, S., & Wang, H. (2019). Cerebellar disruption impairs working memory during evidence accumulation. *Nature Communications*, 10, 3128.

Deverett, B., Koay, S. A., Oostland, M., & Wang, S. S. H. (2018). Cerebellar involvement in an evidence-accumulation decision-making task. *eLife*, 7, e36781.

Dixon, M. L., Thiruchselvam, R., Todd, R., & Christoff, K. (2017). Emotion and the prefrontal cortex: An integrative review. *Psychological Bulletin*, 143(10), 1033.

Dove, A., Pollmann, S., Schubert, T., Wiggins, C. J., & von Cramon, D. Y. (2000). Prefrontal cortex activation in task switching: an event-related fMRI study. *Cognitive Brain Research*, 9(1), 103–109.

Fellows, L. K., & Farah, M. J. (2007). The role of ventromedial prefrontal cortex in decision making: Judgment under uncertainty or judgment per se? *Cerebral Cortex*, 17(11), 2669–2674.

FitzGerald, T. H. B., Seymour, B., & Dolan, R. J. (2009). The role of human orbitofrontal cortex in value comparison for incommensurable objects. *Journal of Neuroscience*, 29(26), 8388–8395.

Foerde, K., Steinglass, J. E., Shohamy, D., & Walsh, B. T. (2015). Neural mechanisms supporting maladaptive food choices in anorexia nervosa. *Nature Neuroscience*, 18(11), 1571–1573.

Fregni, F., Orsati, F., Pedrosa, W., Fecteau, S., Tome, F. A. M., Nitsche, M. A., Mecca, T., Macedo, E. C., Pascual-Leone, A., & Boggio, P. S. (2008). Transcranial direct current stimulation of the prefrontal cortex modulates the desire for specific foods. *Appetite*, 51(1), 34–41.

Fujiwara, J., Usui, N., Eifuku, S., Iijima, T., Taira, M., Tsut-sui, K.-I., & Tobler, P. N. (2018). Ventrolateral prefrontal cortex updates chosen value according to choice set size. *Journal of Cognitive Neuroscience*, 30(3), 307–318.

Jocham, P., Furlong, M., Kroger, I. L., Kahn, M. C., Hunt, L. T., & Behrens, T. E. J. (2014). Dissociable contributions of ventromedial prefrontal and posterior parietal cortex to value-guided choice. *NeuroImage*, 100, 498–506.

Gluth, S., Rieskamp, J., & Buchel, C. (2012). Deciding when to decide: Time-variant sequential sampling models explain the emergence of value-based decisions in the human brain. *Journal of Neuroscience*, 32(31), 10686–10698.

Goel, V., Gold, B., Kapur, S., & Houle, S. (1997). The seats of reason? an imaging study of deductive and inductive reasoning. *Neuroreport*, 8(5), 1305–1310.

Goldberg, T. E., Berman, K. F., Fleming, K., Ostrem, J., Van Horn, J. D., Esposito, G., Mattay, V. S., Gold, J. M., & Weinberger, D. R. (1998). Uncoupling cognitive workload and prefrontal cortical physiology: A pet rcbf study. *Neuroimage*, 7(4), 296–303.

Goni, J., Aznarez-Sanado, M., Arrondo, G., Fernandez-Seara, M., Loayza, F. R., Heukamp, F. H., & Pastor, M. A. (2011). The neural substrate and functional integration of uncertainty in decision making: an information theory approach. *PLoS One*, 6(3), e17408.

Gottwald, B., Wilde, B., Mihajlovic, Z., & Mehdorn, H. M. (2004). Evidence for distinct cognitive deficits after focal cerebellar lesions. *Journal of Neurology, Neurosurgery & Psychiatry*, 75(11), 1524–1531.

Grimaldi, G., & Manto, M. (2012). Topography of cerebellar deficits in humans. *The Cerebellum*, 11(2), 336–351.

Grinband, J., Wager, T. D., Lindquist, M., Ferrera, V. P., & Hirsch, J. (2008). Detection of time-varying signals in event-related fMRI designs. *NeuroImage*, 43(3), 509–520.

Hall, P. A., Lowe, C., & Vincent, C. (2017). Brain stimulation effects on food cravings and consumption: an update on Lowe et al. (2017) and a response to Generoso et al.(2017). *Psychosomatic Medicine*, 79(7), 839–842.

Harbaugh, W. T., Krause, K., & Berry, T. R. (2001). Garp for kids: On the development of rational choice behavior. *American Economic Review*, *91*(5), 1539–1545.

Hare, T. A., Camerer, C. F., & Rangel, A. (2009). Self-control in decision-making involves modulation of the vmPFC valuation system. *Science*, *324*(5927), 646–648.

Hare, T. A., Malmaud, J., & Rangel, A. (2011a). Focusing attention on the health aspects of foods changes value signals in vmPFC and improves dietary choice. *Journal of Neuroscience*, *31*(30), 11077–11087.

Hare, T. A., O'Doherty, J., Camerer, C. F., Schultz, W., & Rangel, A. (2008). Dissociating the role of the orbitofrontal cortex and the striatum in the computation of goal values and prediction errors. *Journal of Neuroscience*, *28*(22), 5623–5630.

Hare, T. A., Schultz, W., Camerer, C. F., O'Doherty, J. P., & Rangel, A. (2011b). Transformation of stimulus value signals into motor commands during simple choice. *Proceedings of the National Academy of Sciences*, *108*(44), 18120–18125.

Harris, A., Hare, T., & Rangel, A. (2013). Temporally dissociable mechanisms of self-control: Early attentional filtering versus late value modulation. *Journal of Neuroscience*, *33*(48), 18917–18931.

He, Q., Huang, X., Zhang, S., Turel, O., Ma, L., & Bechara, A. (2019). Dynamic causal modeling of insular, striatal, and prefrontal cortex activities during a food-specific go/nogo task. *Biological Psychiatry: Cognitive Neuroscience and Neuroimaging*, *4*(12), 1080–1089.

Heekeren, H. R., Marrett, S., Bandettini, P. A., & Ungerleider, L. G. (2004). A general mechanism for perceptual decision-making in the human brain. *Nature*, *431*(7010), 859–862.

Heekeren, H. R., Marrett, S., Ruff, D. A., Bandettini, P. A., & Ungerleider, L. G. (2006). Involvement of human left dorsolateral prefrontal cortex in perceptual decision making is independent of response modality. *Proceedings of the National Academy of Sciences*, *103*(26), 10023–10028.

Henri-Bhargava, A., Simioni, A., & Fellows, L. K. (2012). Ventromedial frontal lobe damage disrupts the accuracy, but not the speed, of value-based preference judgments. *Neuropsychologia*, *50*(7), 1536–1542.

Hunt, L. T., Woolrich, M. W., Rushworth, M. F. S., & Behrens, T. E. J. (2013). Trial-type dependent frames of reference for value comparison. *PLoS Computational Biology*, *9*(9), e1003225.

Hutcherson, C. A., Plassmann, H., Gross, J. J., & Rangel, A. (2012). Cognitive regulation during decision making shifts behavioral control between ventromedial and dorsolateral prefrontal value systems. *Journal of Neuroscience*, *32*(39), 13543–13554.

Jenkinson, M., Beckmann, C. F., Behrens, T. E. J., Woolrich, M. W., & Smith, S. M. (2012). Fsl. *Neuroimage*, *62*(2), 782–790.

Kable, J. W., & Glimcher, P. W. (2007). The neural correlates of subjective value during intertemporal choice. *Nature Neuroscience*, *10*(12), 1625.

Kahnt, T., Heinzle, J., Park, S. Q., & Haynes, J.-D. (2011). Decoding different roles for vmPFC and dlPFC in multi-attribute decision making. *NeuroImage*, *56*(2), 709–715.

Karatekin, C., Lazareff, J. A., & Asarnow, R. F. (2000). Relevance of the cerebellar hemispheres for executive functions. *Pediatric Neurology*, *22*(2), 106–112.

Kim, H., Shimojo, S., & O'Doherty, J. P. (2010). Overlapping responses for the expectation of juice and money rewards in human ventromedial prefrontal cortex. *Cerebral Cortex*, *21*(4), 769–776.

Konovalov, A., & Krajbich, I. (2019). Over a decade of neuroeconomics: What have we learned? *Organizational Research Methods*, *22*(1), 148–173.

Koob, G. F., & Volkow, N. D. (2010). Neurocircuitry of addiction. *Neuropsychopharmacology*, *35*(1), 217–238.

Kroger, J. K., Sabb, F. W., Fales, C. L., Bookheimer, S. Y., Cohen, M. S., & Holyoak, K. J. (2002). Recruitment of anterior dorsolateral prefrontal cortex in human reasoning: A parametric study of relational complexity. *Cerebral Cortex*, *12*(5), 477–485.

Lee, S., Linda, Q. Y., Lerman, C., & Kable, J. W. (2021). Subjective value, not a gridlike code, describes neural activity in ventromedial prefrontal cortex during value-based decision-making. *NeuroImage*, *237*, 118159.

Levy, D. J., & Glimcher, P. W. (2011). Comparing apples and oranges: Using reward-specific and reward-general subjective value representation in the brain. *Journal of Neuroscience*, *31*(41), 14693–14707.

Levy, D. J., & Glimcher, P. W. (2012). The root of all value: A neural common currency for choice. *Current Opinion in Neurobiology*, *22*(6), 1027–1038.

Lim, S.-L., O'Doherty, J. P., & Rangel, A. (2011). The decision value computations in the vmPFC and striatum use a relative value code that is guided by visual attention. *Journal of Neuroscience*, *31*(37), 13214–13223.

Lim, S.-L., O'Doherty, J. P., & Rangel, A. (2013). Stimulus value signals in ventromedial PFC reflect the integration of attribute value signals computed in fusiform gyrus and posterior superior temporal gyrus. *Journal of Neuroscience*, *33*(20), 8729–8741.

Lowe, C. J., Reichelt, A. C., & Hall, P. A. (2019). The prefrontal cortex and obesity: A health neuroscience perspective. *Trends in Cognitive Sciences*, *23*(4), 349–361.

Luo, S., Ainslie, G., Pollini, D., Giragosian, L., & Monterosso, J. R. (2012). Moderators of the association between brain activation and farsighted choice. *NeuroImage*, *59*(2), 1469–1477.

Manes, F., Villamil, A. R., Ameriso, S., Roca, M., & Torralva, T. (2009). "Real life" executive deficits in patients with focal vascular lesions affecting the cerebellum. *Journal of the Neurological Sciences*, *283*(1–2), 95–98.

Matějka, F., & McKay, A. (2015). Rational inattention to discrete choices: A new foundation for the multinomial logit model. *American Economic Review*, *105*(1), 272–298.

McClure, S. M., Li, J., Tomlin, D., Cypert, K. S., Montague, L. M., & Montague, P. (2004). Neural correlates of behavioral preference for culturally familiar drinks. *Neuron*, *44*(2), 379–387.

McFadden, B. R., Lusk, J. L., Crespi, J. M., Bradley, J., Cherry, C., Martin, L. E., Aupperle, R. L., & Bruce, A. S. (2015). Can neural activation in dorsolateral prefrontal cortex predict responsiveness to information? an application to egg production systems and campaign advertising. *PLoS One*, *10*(5), e0125243.

McFadden, D. (1973). Conditional logit analysis of qualitative choice behavior. In P. Zarembka (Ed.), *Frontiers in Econometrics*. Academic Press. pp. 105–142.

Monterosso, J. R., Ainslie, G., Xu, J., Cordova, X., Domier, C. P., & London, E. D. (2007). Frontoparietal cortical activity of methamphetamine-dependent and comparison subjects performing a delay discounting task. *Human brain Mapping*, *28*(5), 383–393.

Nakamura-Palacios, E. M., Lopes, I. B. C., Souza, R. A.-q., Klauss, J., Batista, E. K., Conti, C. L., Moscon, J. A.-d., & de Souza, R. S. M. (2016). Ventral medial prefrontal cortex (vmpfc) as a target of the dorsolateral prefrontal modulation by transcranial direct current stimulation (tdcs) in drug addiction. *Journal of Neural Transmission*, *123*(10), 1179–1194.

Nichelli, P., Grafman, J., Pietrini, P., Alway, D., Carton, J. C., & Miletich, R. (1994). Brain activity in chess playing. *Nature*, *369*, 191.

O'Doherty, J. P., Buchanan, T. W., Seymour, B., & Dolan, R. J. (2006). Predictive neural coding of reward preference involves dissociable responses in human ventral midbrain and ventral striatum. *Neuron*, *49*(1), 157–166.

Osherson, D., Perani, D., Cappa, S., Schnur, T., Grassi, F., & Fazio, F. (1998). Distinct brain loci in deductive versus probabilistic reasoning. *Neuropsychologia*, *36*(4), 369–376.

Pelletier, G., Aridan, N., Fellows, L. K., & Schonberg, T. (2021). A preferential role for ventromedial prefrontal cortex in assessing "the value of the whole" in multiattribute object evaluation. *Journal of Neuroscience*, *41*, 5056–5068.

Petrides, M. (1994). Frontal lobes and behaviour. *Current Opinion in Neurobiology*, *4*(2), 207–211.

Plassmann, H., O'Doherty, J., & Rangel, A. (2007). Orbitofrontal cortex encodes willingness to pay in everyday economic transactions. *Journal of Neuroscience*, *27*(37), 9984–9988.

Poldrack, R. A. (2015). Is "efficiency" a useful concept in cognitive neuroscience? *Developmental Cognitive Neuroscience*, *11*, 12–17.

Rangel, A., Camerer, C., & Montague, P. R. (2008). A framework for studying the neurobiology of value-based decision making. *Nature Reviews Neuroscience*, *9*(7), 545.

Rosenbloom, M. H., Schmahmann, J. D., & Price, B. H. (2012). The functional neuroanatomy of decision-making. *The Journal of Neuropsychiatry and Clinical Neurosciences*, *24*(3), 266–277.

Rudorf, S., & Hare, T. A. (2014). Interactions between dorsolateral and ventromedial prefrontal cortex underlie context-dependent stimulus valuation in goal-directed choice. *Journal of Neuroscience*, *34*(48), 15988–15996.

Serences, J. T. (2008). Value-based modulations in human visual cortex. *Neuron*, *60*(6), 1169–1181.

Serences, J. T., & Saproo, S. (2010). Population response profiles in early visual cortex are biased in favor of more valuable stimuli. *Journal of Neurophysiology*, *104*(1), 76–87.

Shevlin, B. R. K., Smith, S. M., Hausfeld, J., & Krajbich, I. (2022). High-value decisions are fast and accurate, inconsistent with diminishing value sensitivity. *Proceedings of the National Academy of Sciences*, *119*(6), e2101508119.

Sokol-Hessner, P., Hutcherson, C., Hare, T., & Rangel, A. (2012). Decision value computation in dlPFC and vmPFC adjusts to the available decision time. *European Journal of Neuroscience*, *35*(7), 1065–1074.

Tang, D. W., Fellows, L. K., Small, D. M., & Dagher, A. (2012). Food and drug cues activate similar brain regions: A meta-analysis of functional MRI studies. *Physiology & Behavior*, *106*(3), 317–324.

Teodorescu, A. R., Moran, R., & Usher, M. (2016). Absolutely relative or relatively absolute: Violations of value invariance in human decision making. *Psychonomic Bulletin & Review*, *23*(1), 22–38.

Train, K. E. (2009). *Discrete choice methods with simulation*. Cambridge University Press.

Weiskopf, N., Hutton, C., Josephs, O., & Deichmann, R. (2006). Optimal epi parameters for reduction of susceptibility-induced bold sensitivity losses: A whole-brain analysis at 3t and 1.5t. *NeuroImage*, *33*(2), 493–504.

SUPPORTING INFORMATION

Additional supporting information can be found online in the Supporting Information section at the end of this article.